Published in final edited form as:

Mol Cancer Ther. 2016 September ; 15(9): 2107–2118. doi:10.1158/1535-7163.MCT-16-0241.

Co-targeting HSP90 and its client proteins for treatment of prostate cancer

Long Chen[1], **Jie Li**[1], **Elia Farah**[1], **Sukumar Sarkar**[2], **Nihal Ahmad**[3], **Sanjay Gupta**[4], **James Larner**[2], and **Xiaoqi Liu**[1,5,*]

[1]Department of Biochemistry, Purdue University, West Lafayette, IN 47907

[2]Department of Radiation Oncology, University of Virginia, Charlottesville, VA 22908

[3]Department of Dermatology, University of Wisconsin, Madison, WI 53706

[4]Department of Urology, Case Western Reserve University, Cleveland, OH 44106

[5]Center for Cancer Research, Purdue University, West Lafayette, IN 47907

Abstract

Castration-resistant prostate cancer (CRPC) is the later stage of prostate cancer (PCa) when the disease has stopped responding to androgen deprivation therapy (ADT). It has been established that androgen receptor (AR) re-activation is responsible for the recurrence of PCa after ADT. Thus targeting different pathways that regulate AR stability and activity should be a promising strategy for treatment of CRPC. Heat shock proteins (HSPs) are chaperones that modify stability and activity of their client proteins. HSP90, a major player of the HSP family, regulates stabilities of many proteins, including AR and Polo-like kinase 1 (Plk1), a critical regulator of many cell cycle events. Further, HSP90 is overexpressed in different cancers, including PCa. Herein, we show that co-treatment of PCa with AR antagonist enzalutamide and HSP90 inhibitor leads to more severe cell death due to a synergistic reduction of AR protein. Interestingly, we show that overexpression of Plk1 rescued the synergistic effect and that co-targeting HSP90 and Plk1 also leads to more severe cell death. Mechanistically, we show that E3 ligase CHIP, in addition to targeting AR, is responsible for the degradation of Plk1 as well. These findings suggest that co-targeting HSP90 and some of its client proteins may be a useful strategy in treatment of CRPC.

Keywords

HSP90; AR; Plk1; Enzalutamide; 17-AAG

Introduction

Androgen plays pivotal roles in the progression of prostate cancer (PCa) (1), the second most commonly diagnosed cancer among man worldwide (2). Accordingly, androgen

*Corresponding Author: To whom correspondence should be addressed: Department of Biochemistry, Purdue University, 175 S. University Street, West Lafayette, IN 47907 Tel: 765-496-3764; Fax: 765-494-7897; liu8@purdue.edu.

Disclosure of Potential Conflicts of Interest: No potential conflicts of interest are disclosed by the authors.

deprivation therapy (ADT), which blocks androgen production or action through either physical castration or chemical castration, is the first line treatment for locally advanced or metastatic PCa (3-5). Despite the early success of ADT, the disease eventually relapses and enters a stage called castration-resistant prostate cancer (CRPC) (5). Most biological functions of androgens are mediated by androgen receptor (AR), a ligand-dependent transcription factor that regulates gene expression of the androgen-dependent signaling components (6). AR initially localizes in the cytoplasm in a complex with heat shock proteins (HSPs), cytoskeletal proteins and co-chaperone proteins. Upon binding to androgens, AR translocates into the nucleus, where it binds to the androgen response elements (ARE) in the promoter or enhancer regions of targeted genes with other co-activators and activates the androgen signaling pathway (6). It has been established that re-activation of AR signaling is responsible for relapse of PCa (7, 8). Consequently, drugs targeting AR pathway such as enzalutamide have been used for CRPC patients. Although the drug provides a substantial survival benefit, patients develop enzalutamide resistance eventually due to re-activation of AR (9). Thus, new strategies targeting the AR signaling pathway are needed to overcome enzalutamide resistance.

HSPs are chaperone proteins that are expressed during stress and facilitate the stabilization, folding and translocation of its client proteins (10). HSP90, a member of the HSP family, functions to stabilize and activate its client proteins in an ATP-dependent manner (11). HSP90 has more than 200 client proteins, which are involved in different signaling pathways and adaptive response to stress. HSP90 clients include oncogenic proteins, such as v-Src, Bcr-Abl, c-Met and Plk1 (12, 13). Thus, inhibition of HSP90 has been considered a promising way for cancer treatment. In PCa, HSP90 regulates the stability and activity of AR by forming a complex with AR in the cytoplasm thus stabilizing AR prior to ligand binding (14). Inhibition of HSP90 leads to AR degradation and its cytoplasmic accumulation (15, 16). Most of HSP90 inhibitors developed so far target the ATP-binding domain of HSP90, leading to its inactivation and eventually degradation of its client proteins (11), with Geldanamycin (GA) as one of the such HSP90 inhibitors (16-18). Although GA has been shown to be effective in many cell lines, it did not enter clinical trials due to its severe liver cytotoxicity (11). 17-Allylamino-17-demethoxy- geldanamycin (17-AAG), a GA derivative, which also shows antitumor activity but less cytotoxicity in vivo, was the first HSP90 inhibitor that entered clinical trials (12, 19, 20). Unfortunately, due to lack of response and toxicity, the phase II studies in patents with breast cancer and melanoma were terminated early (21, 22). Despite these, newly developed HSP90 inhibitors with higher specificity and less toxicity, such as AUY922 and STA-9090, are now in different clinical trials, and combination therapies of Hsp90 inhibitors with standard chemotherapy or radiotherapy are ongoing (11, 20, 23).

Polo-like kinase 1 (Plk1) is a serine/threonine kinase that has many cell cycle-related functions (24). Plk1, overexpressed in many human tumors, including PCa, has been preclinically validated as a target for cancer treatment (25). While inhibitors of Plk1 are in different clinical trials, we recently reported that inhibition of Plk1 potentiated enzalutamide-mediated therapy in CRPC (26). Moreover, HSP70 and HSP90 have been shown to bind to Plk1 and regulate its function (27-29).

C-terminal Hsc70-interacting protein (CHIP) is a co-chaperone protein that works with chaperone proteins (HSP70/90) to modulate the protein homeostasis, either facilitating the unfolded or damaged proteins fold properly or directing those proteins to go through the proteasome-mediated degradation (30-32). CHIP itself is an E3 ubiquitin ligase, therefore, its binding to HSPs leads to degradation of client proteins (32). While CHIP binds and regulates the degradation of AR (33-35), it is a Plk1-interacting protein during mitosis as well (36).

By combining HSP90 inhibitors with drugs targeting HSP90 client proteins like AR or Plk1 in PCa, we showed that combination of HSP90 inhibitors with AR or Plk1 inhibitors led to cell death in a synergistic manner, providing a novel approach to treat CRPC. Mechanistically, CHIP-mediated degradation of AR and Plk1 leads to enhanced efficacy of HSP90 inhibitors.

Materials and Methods

Cell culture, Virus infection and Drugs

HEK293T, HeLa, LNCaP and 22RV1 cells were purchased from American Type Culture Collection. Cells were grown and aliquots were stored in liquid nitrogen for future use. Cells were purchased more than 6 months ago and were not further tested or authenticated by authors. HEK293T and Hela cells were cultured in Dulbecco modified Eagle Medium (DMEM) (Sigma) supplemented with 10% fetal bovine serum (FBS) (Atlanta), 80 mM L-glutamine (Sigma) and 100 units/ml penicillin, 100 units/ml streptomycin at 37°C in 5% CO2. Prostate Cancer cell line LNCaP and C4-2 were cultured in RPMI 1640 Medium (Sigma) supplemented with 10% FBS and 100 units/ml penicillin, 100 units/ml streptomycin at 37 °C in 5% CO2. Enzalutamide-resistant prostate cancer cell line 22RV1 and MR49F were also cultured in RPMI 1640 Medium with 10% FBS and 100 units/ml penicillin, 100 units/ml streptomycin, with 10 nM enzalutamide to maintain resistance at 37 °C in 5% CO2. C4-2 and MR49F cells were general gifts from Dr. Amina Zoubeidi from University of British Columbia. Cells were grown and aliquots were stored in liquid nitrogen for future use and were not tested or authenticated by authors. Virus carrying CHIP shRNA was described previously.(37) Virus solution was added into growth medium together with polybrene and Hepes. Geldanamycin, Nocodazole and MG132 were purchased from Sigma-Aldrich. Enzalutamide and 17-AAG were purchased from Medchem Express and Reagents Direct, respectively. BI2536 were Purchased from Symansis NZ Ltd, New Zealand. Structure of drugs were included in Supplementary Methods and Materials.

Protein Purification

After indicated domains of CHIP or Plk1 were PCR amplified and subcloned into pGEX-KG, glutathione-S-transferasae (GST)-tagged CHIP and GST-Plk1 proteins were expressed in Escherichia coli and purified using GST-agarose beads.

Antibodies

Antibodies against Plk1 (sc-17783), HSP90 (sc-13119) and ubiquitin (sc-8017) were purchased from Santa Cruz Biotech. Antibodies against β-actin (A-5441), Cyclin B

(554177), and cleaved-PARP (AB6535) were obtained from Sigma, BD Pharmingen, and EMD Millipore, respectively. All other antibodies were purchased from Cell Signaling.

Immunoblotting (IB) and Immunoprecipitation (IP)

Upon harvest, cells were re-suspended with TBSN buffer with protease inhibitors and phosphatase inhibitors and sonicated. After were collected, protein concentrations were measured using Protein Assay Dye Reagent from Bio-Rad. Equal amounts of protein from each sample were mixed with SDS loading buffer and resolved by SDS-PAGE. Upon transferring to PVDF membranes, proteins were probed with indicated antibodies. For IP, cell lysates were incubated with indicated antibodies overnight at 4°C, followed by 1 hr of incubation with protein A/G plus-Agarose beads. After supernatants were removed, beads were washed with high salt and low salt TBSN buffer, and resolved by SDS-PAGE.

GST pull down assay

After GST-fusion CHIP proteins were expressed and enriched using GST agarose beads, cell lysates were incubated with the GST beads carrying the proteins at 4°C overnight. After centrifugation, supernatants were removed and beads were washed three time and resolved by SDS-PAGE for Coomassie brilliant blue staining or Western blot detection.

In vitro ubiquitination assay

In vitro ubiquitination assay was performed using CHIP Ubiquitin Ligase Kit purchased from Boston Biochem. Briefly, GST-Plk1 proteins purified from E.coli were incubated with the reaction buffer containing Mg^{2+}-ATP and HSP70/HSP40 at 43°C for 7 min and kept on ice for 10 min. Then, addition of E1, E2 and CHIP were followed by ubiquitin to the mixture. Samples were placed at 37°C and incubated for indicated times until termination with SDS loading buffer.

Chromatin Immunoprecipitation

Upon harvest with trypsin, cells were crosslinked with 1% formaldehyde and quenched with glycine. Nuclear fraction was separated and re-suspended in SDS lysis buffer (10 mM Tris-HCl pH7.5, 150 mM NaCl, 0.5% SDS, 1 mM EDTA, supplemented with protease inhibitors and phosphatase inhibitors). Sonication was used to shear DNA into desired lengths. Upon centrifugation, supernatants were collected and incubated with AR antibody and protein A/G agarose beads. After several washes, chromatin complexes were eluted with elution buffer (1% SDS, 0.1 M NaHCO3), crosslinking was reserved by incubating the eluted chromatin complexes at 65°C overnight. RNase A and proteinase K were then added and incubated at 37°C for 1 hour. After DNA was isolated using PCR purification kit from Qiagen, DNA binding to AR was measured by RT-PCR. PCR Results were normalized to indicated DNA in the supernatants.

Immunofluorescence (IF)

Cells were grown on coverslips under normal culture conditions, fixed with 4% formaldehyde, and blocked with 5% bovine serum albumin (BSA) for 1 hr. Primary and

secondary antibodies were prepared in 5% BSA and incubated on coverslips for 2 hr and 1hr, respectively.

Xenograft study

Mice carrying LuCaP35CR tumors were obtained from Dr. Robert Vessella from University of Washington. 24 mice carrying LuCaP35CR tumor were used for study. When tumors reached around 200 mm^3, mice were separated into 4 groups for indicated treatments. For the first two weeks, enzalutamide (25 mg/kg) was gavaged twice per week and 17-AAG (20 mg/kg) was intraperitoneally injected twice per week. Starting from the third week, both drugs were administered 5 times a week. Tumor volumes were measured by formula $V=L \times W^2/2$ (V is volume [mm^3], L is length [mm], W is width [mm]). Mice were sacrificed when the volume of one or more tumors reached 1000mm^3.

Hematoxylin and eosin (H&E) staining and Immunohistochemistry (IHC) staining

Tumors were fixed in 10% formalin, embedded in paraffin, sectioned and subjected for H&E staining. IHC and IF staining were performed by using VECTASTAIN ABC Kit from Vector Laboratories.

Cell viability assay

Cells were seeded in 96-well plates, treated with indicated drugs for 3 days, and subjected for CellTiger-Glo luminescent cell viability assay kit from Promega.

Subcellular fractionation

Cytoplasmic and nuclear fractions of cells were prepared using Nuclear Extract Kit from Active Motif. Briefly, harvested cells were re-suspended in hypotonic buffer, vortexed for 10 s, and centrifuged for 30 s at 14,000 rpm at 4°C. Supernatants were collected as cytoplasmic fraction. Nuclear pellets were re-suspended using complete lysis buffer, incubated on ice for 30 min, vortexed for 30 s, and centrifuged for 10 min at 14,000 rpm. Supernatants were collected as nuclear fraction.

Results

Combination of HSP90 inhibitors with AR antagonist enzalutamide induces an increased cell death and decreased cell viability in PCa cell lines. It has been shown that HSP90 inhibitor 17-AAG works synergistically with AR antagonist bicalutamide to suppress PCa cell growth (38). Enzalutamide is a newly developed AR antagonist that has been approved by the US Food and Drug Administration (FDA) to treat metastatic CRPC in 2014. By preventing androgen binding to AR, enzalutamide inhibits the nuclear localization and transcriptional activity of AR (39). Despite the early clinical benefits, most patients eventually developed enzalutamide resistance due to reactivation of the AR signaling pathway by various mechanisms including AR truncation and point mutations (9). Here, three different PCa cell lines were used to test whether HSP90 inhibitors (17-AAG and GA) would sensitize cells to enzalutamide treatment. Both C4-2 and 22RV1 are CRPC cells, with the later to be enzalutamide resistant as well. Like C4-2, MR49F cells are also derived from LNCaP cells but enzalutamide resistant (37). C4-2, 22RV-1, MR49F cells were treated with

enzalutamide, HSP90 inhibitor or together, followed by various analyses. Decreased cell viability and increased cell death upon combination treatment were observed in all three cell lines (Fig. 1A-1D). Enzalutamide-resistant 22RV1 and MR49F cells were also treated with increased concentrations of 17-AAG in the presence of enzalutamide (Fig. 1E and 1F). 17-AAG-induced apoptosis of 22RV1 and MR49F cells is apparently dose dependent, suggesting that HSP90 inhibitor is effective in treating enzalutamide-resistant CRPC. At the same time, the decrease of AR protein level was also observed as the concentration of 17-AAG is increased (Fig. 1E and 1F).

Co-treatment with HSP90 inhibitor and enzalutamide leads to AR protein degradation, nuclear exclusion and decreased transcription activity. HSP90 inhibitors cause degradation of AR protein and its nuclear exclusion, whereas AR antagonist like enzalutamide also inhibits AR nuclear localization thus its transcriptional activity. We examined the AR protein level, nuclear localization and transcriptional activity upon co-treatment of LNCaP, C4-2, 22RV1 and MR49F cells with enzalutamide and HSP90 inhibitor. Upon combining the two drugs, AR protein levels are further decreased, as well as the levels of prostate specific antigen (PSA), the major AR downstream target (Fig. 2A-2D). Enhanced expression of truncated version of AR (AR-V) in 22RV1 cells is one established mechanism for enzalutamide resistance (40). Of interest, combination of GA and enzalutamide almost completely abolished the expression of both full-length AR and AR-V in 22RV1 cells (Fig. 2C). We noticed that there is an increase of AR protein level in 22RV1 and MR49F cells upon enzalutamide treatment (Fig. 2B, 2C). Although we maintained enzalutamide resistance of the two cell lines by adding enzalutamide when sub-culturing, we did not add enzalutamide when we seeded the cells for treatments, so it is possible that the two cell lines overcome enzalutamide partially by overexpressing AR protein. The effects of two drug combination on AR localization were then analyzed by immunofluorescence (IF) staining (Fig. 3). For LNCaP and C4-2 cells, both enzalutamide and GA treatment lead to increased AR localization in the cytoplasm, while enzalutamide shows less effect (Fig. 3A and 3B). Upon co-treatment with both enzalutamide and GA, cells showed diffused cytosolic AR pattern and reduced total AR signal as well. The effects of enzalutamide plus GA on AR localization in two enzalutamide-resistant lines were also examined. While enzalutamide alone had little impact on AR nuclear localization in both lines, additional GA treatment clearly reduced both total total AR level and its nuclear localization (Fig. 3C and 3D). The different responses of two lines to the combinational treatment needs further experimentation. To further test the localization of AR upon different drug treatments, C4-2 cells treated with enzalutamide and 17-AAG were subjected to cell fractionation. While the cytosolic AR was reduced by the combinational treatment, a much more significant decrease was observed in the nuclear AR upon the treatment by enzalutamide plus 17-AAG (Fig. 2E). AR binding to the chromatin upon drug treatment was examined. Accordingly, C4-2 cells were treated with various conditions for 24 hr, crosslinked with formaldehyde, and harvested for chromatin isolation. Samples were subjected to anti-histone H3 immunoprecipitation (IP), followed by anti-AR IB. While chromatin-loading of AR was not significantly affected by two single drug treatments, combining the two drugs leads to a reduced AR binding to chromatin (Fig. 2F). CHIP was also performed to further confirm binding of AR to the promoter region of its target genes upon drug treatment. C4-2 cells were treated as indicated

for 24 hr and subjected for CHIP analysis. Binding of AR to promoter region of PSA, CAMKK2 and FKBP5 were analyzed using RT-PCR with specific primers targeting the promoter region of indicated genes. Although either single drug treatment could decrease the binding of AR to the promoter region of these target genes compared with control group, combination treatment was more effective in inhibiting AR binding to the promoter region of the three target genes than single drug treatment (Fig. 2G).

17-AAG enhances the efficacy of enzalutamide in vivo. We next tested the effect of combination of enzalutamide and 17-AAG in the LuCaP35CR patient-derived xenograft (PDX) model. While 17-AAG alone showed a better effect than enzalutamide alone, combination of enzalutamide and 17-AAG led to a more significantly decreased tumor growth rate compared with single drug treatments (Fig. 4A and 4B). Histological analyses of the harvested tumors were performed to further characterize the drug effect. H&E staining indicated necrosis the interior tumors, consequently we mainly analyzed the exterior of the tumors where cells were still actively growing (data not shown). While single drug treatments did not lead to significant change of tumor grade and morphology compared with the control group, combination treatment led to increased apoptotic bodies and condensed nuclear pyknosis (Fig. 4C, top panel). Combination of the two drugs also led to a significantly decreased proliferation rate of the tumor cells as indicated by Ki67 staining (Fig. 4C and 4D). The PSA level in the serum was also decreased upon combination compared with single drug treatments, indicating that the transcriptional activity of AR was inhibited (Fig. 4E). Consistent with our results using cell lines, AR tended to be excluded from the nucleus and total AR signal intensity was decreased upon combination treatment in the xenograft model (Fig. 4F).

AR protein level upon drug treatment is partially dependent on CHIP. CHIP, a co-chaperone protein that works with chaperone proteins like HSPs to regulate protein hemostasis, is also an E3 ubiquitin ligase. It has been established that proteins with critical roles in cell signaling and cancer progression, such as p53, HIF1a and Smad, are ubiquitinated and regulated by CHIP (35, 41-43). Of significance, AR is also degraded by CHIP (35). Thus, we asked whether CHIP plays a regulatory role in the HSP90 inhibition-induced AR degradation by depleting CHIP in 22RV1 cells. CHIP was depleted in 22RV1 and MR49F cells by infection with lentivirus containing shRNA targeting CHIP, followed by puromycin selection. Control or CHIP-depleted cells were treated with GA for indicated times and subjected for western blot to detect AR protein level (Fig. 5A, B). GA treatment-induced degradation of AR was clearly delayed upon CHIP depletion in MR49F cells and for the AR-V in 22RV1 cells, suggesting that CHIP is partially responsible for the degradation of AR protein upon HSP90 inhibition.

Plk1 inhibition potentiates HSP90 inhibition-induced apoptosis in PCa cells. Next, CHIP-depleted 22RV1 cells were treated with enzalutamide, followed by IB against C-PARP and Plk1. While enzalutamide did not significantly affect cell death due to CHIP depletion, it clearly elevated the level of Plk1, in particular, in CHIP-depleted cells, suggesting that Plk1 might be also involved in the efficacy of HSP90 inhibitors (Fig. 5C). Of note, we previously showed that enzalutamide and Plk1 inhibitor BI2536 act synergistically to induce apoptosis in CRPC (26). Considering that Plk1 is also a client protein of HSP90, we asked whether

Plk1 affects the synergistic effect of HSP90 inhibitor and enzalutamide. As indicated, Plk1 overexpression indeed abolished the synergistic effect of enzalutamide and GA in LNCaP cells (Fig. 5D). We also performed cell viability assay on cells overexpressing Plk1 upon different treatments. While combination treatment led to decreased cell viability, overexpression of Plk1 abolished the combination effect, which is consistent with our western result (Fig S1) . Furthermore, inhibition of Plk1 with BI2536 clearly potentiated 17-AAG-induced apoptosis in LNCaP, 22RV-1 and MR49F cells (Fig. 5E-5G). To dissect the underlying mechanism, we showed that 17-AAG-mediated HSP90 inhibition led to significant decrease of the protein levels of Plk1 in LNCaP, C4-2 and MR49F cells (Fig. 5H-5J). Therefore, HSP90 inhibition results in Plk1 degradation.

CHIP is an E3 ubiquitin ligase of Plk1. Because we observed an increase of Plk1 protein level upon CHIP depletion (Fig. 5C), and because CHIP itself is an E3 ubiquitin ligase, we tested whether CHIP can directly ubiquitinate Plk1. Accordingly, HEK293T cells were co-transfected with Flag-CHIP, GFP-Plk1 and His-ubiquitin, treated cells with GA, and harvested for anti-Plk1 immunoprecipitation (IP), followed by IB against ubiquitin. Consistent with reduced protein level of Plk1 upon HSP90 inhibition, GA treatment led to an increased level of ubiquitination of Plk1 (Fig. 5H). Next, HeLa cells, pre-treated with or without nocodazole, were depleted of CHIP and analyzed for anti-Plk1 IB. Upon CHIP knockdown, a clear increase of Plk1 protein level was observed in both randomly growing and mitotically arrested cells (Fig. 5L and 5M). Since Plk1 is a mitotic kinase and its protein level is strictly regulated through the cell cycle, we tested whether CHIP depletion would affect the cell cycle distribution. CHIP depletion did not significantly affect the cell cycle progression of HeLa and MR49F cells compared with corresponding control cells as indicated by FACS analysis (Fig. 5N and 5O). Moreover, we showed that overexpression of CHIP in HEK293T cells decreased the level of Plk1 protein and that addition of proteasome inhibitor MG132 rescued the phenotype, further suggesting that CHIP might be responsible for the degradation of Plk1 (Fig. 5M).

To further test whether CHIP is an E3 ubiquitin ligase of Plk1, we asked whether Plk1 binds to CHIP directly. Either randomly growing or nocodazole-treated HeLa cells were subjected to IP with antibodies against Plk1 or CHIP, followed by Western blot analysis. Co-IP experiments indicate that the two proteins interact with each other and that the interaction increases during mitosis (Fig. 6A). GST pull down assay was used to further confirm the interaction. Accordingly, GST-tagged CHIP proteins (two fragments and full length) were expressed in E.coli, enriched on GST beads, and incubated with HeLa cell lysates. After extensive washing, the beads were subjected to anti-Plk1 Western blotting or Coomassie brilliant blue staining. As indicated in Fig. 6B, both N-terminal and C-terminal as well as the full length CHIP bind to Plk1 with N terminus showing a higher binding affinity. To test whether CHIP can directly ubiquitinate Plk1, in vitro ubiquitination assay was performed. In this assay, purified Plk1 was incubated with E1, E2 and CHIP under different conditions. While absence of CHIP prevented ubiquitination of Plk1, addition of CHIP clearly increased ubiquitination of Plk1 in a time-dependent manner (Fig. 6C). In addition, the ubiquitination of Plk1 did not depend on the kinase activity of Plk1 itself, as the kinase-dead mutant Plk1-K82M was also ubiquitinated by CHIP in vitro (Fig. 6D). To further characterize the CHIP-mediated ubiquitination of Plk1, in vitro ubiquitination assay was performed with three

different Plk1 regions. As indicated in Fig. 6E, all three Plk1 fragments were ubiquitinated by CHIP, suggesting that CHIP targets multiple sites of Plk1 for ubiquitination. Next, to test whether Plk1 is ubiquitinated by CHIP in cells, HEK293T cells were co-transfected with Flag-CHIP, GFP-Plk1 and His-ubiquitin, arrested at mitosis with nocodazole, treated with MG132 to inhibit protein degradation, and harvested for anti-Plk1 IP, followed by anti-ubiquitin IB. Overexpression of Flag-CHIP significantly increased ubiquitination of GFP-Plk1, suggesting that CHIP targets Plk1 in cells (Fig. 6F). Finally, the ubiquitination of endogenous Plk1 upon CHIP overexpression was assessed by transfecting Flag-CHIP and His-ubiquitin into HEK293T cells treated with nocodazole and MG132. Again, overexpression of CHIP significantly increased the ubiquitination of endogenous Plk1 (Fig. 6G). Therefore, we concluded that CHIP is an E3 ubiquitin ligase of Plk1 in cells.

Discussion

AR signaling inhibitors like enzalutamide are the major drugs for CRPC treatment with limited success. Thus, it is urgently needed to identify new targets and develop novel approaches to increase the efficiency of enzalutamide. HSPs have important roles in regulating the homeostasis of its client proteins, including AR and Plk1. Indeed, a co-IP experiment indicated a complex formation among HSP90, AR and Plk1 and inhibition of HSP90 led to dissociation of AR and Plk1 from HSP90 (Fig. 7A). Inhibition of HSP90 leads to protein degradation and nuclear exclusion of AR, thus targeting HSP90 is one promising approach in treating PCa. Besides AR, inhibition of HSP90 may also lead to degradation of its other client proteins, eventually contributing to inhibition of cancer cells by providing a broader spectrum of inhibition.

In this study, we first tested combining HSP90 inhibitors GA or 17-AAG with AR inhibitor enzalutamide in cultured PCa cells. Co-targeting HSP90 and AR led to more severe cell death in different PCa cell lines, including the androgen-dependent LNCaP, androgen-independent C4-2, and enzalutamide-resistant 22RV1 and MR49F cells (Fig. 1 and 2). The combination led to increased AR protein degradation, decreased AR nuclear localization and reduced AR transcriptional activity (Fig. 2 and 3). It is of clinical significance for 22RV1 and MR49F cells to respond to the combination treatment, as these cell lines have acquired enzalutamide resistance via different mechanisms such as increased expression of AR-V or point mutations. Although inhibition of HSP90 is expected to lead to degradation of its client proteins, it is not clear why combination of AR antagonist with HSP90 inhibitor would lead to further degradation of AR, especially in those resistant cell lines. Importantly, we found combination of enzalutamide and 17-AAG led to inhibition of tumor growth of a PDX model LuCaP35CR (Fig. 4). We also noticed that upon single drug treatment, 17-AAG is more effective in causing cancer cell death and tumor volume reduction, whereas it is not as effective as enzalutamide in downregulating AR protein level (Fig 1, 2, 4). Since inhibition of HSP90 could lead to degradation of its multiple client proteins, AR is one of many HSP90 clients that are degraded upon 17-AAG treatment. Other HSP90 client proteins, including Plk1, EGFR and HIF1a, are also degraded upon 17-AAG treatment (29, 44, 45), resulting in even severe cancer cell death and tumor volume reduction. Although we found that downregulation of AR upon combination of HSP90 inhibitor and enzalutamide is one of the reasons for increased cancer cell death, it is possible that modulation of other

signaling pathways due to HSP90 inhibition also synergizes with inhibition of AR pathway, eventually resulting in increased cell death. This possibility needs further investigation as it might provide evidence for new combination therapy.

We further found that the HSP90 inhibition-induced AR degradation is partially dependent on CHIP, an E3 ligase that works with chaperone proteins like HSPs to regulate the homeostasis of client proteins (Fig. 5A). Acting as a co-chaperone, CHIP directs client proteins of HSPs for proteasome degradation. However, one report showed binding of CHIP to different HSPs might lead to different destination of client proteins. When CHIP binds to HSP70, it leads to protein degradation. In striking contrast, CHIP can stabilize the client protein when it binds to HSP90 (32, 46). Thus, it is possible that inhibition of HSP90 leads to increased binding of client proteins with HSP70/CHIP complex thus resulting in their degradation.

Interestingly, the protein level of Plk1 was also increased upon CHIP depletion, suggesting that Plk1 might be a CHIP substrate. We then demonstrated this important finding by a series of in vitro and in cell ubiquitination assays (Fig. 6). It has been reported that Plk1 can be ubiquitinated by other E3 ubiquitin ligases. E3 ligase Chfr ubiquitination of Plk1 results in a delay of cells entering mitosis in the presence of mitotic stress through negative regulation of Cdc2 activation (47). Ubiquitination of Plk1 by Cullin 3 ligase complex with the BTB adaptor KLHL22 directs Plk1 dissociation from the kinetochore without affecting Plk1 stability (48, 49). Although CHIP depletion did not affect cell cycle progression during non-stress condition (Fig. 5N and 5O), HSP90 and CHIP are chaperone proteins that are responsible for protein fate during stress. Therefore, it is possible that CHIP-dependent Plk1 ubiquitination would affect cell cycle progression when cells are under stress, similar to Chfr. We hypothesize that when cells are depleted of CHIP, Plk1 cannot be efficiently ubiquitinated under stress, consequently cells continue to cycle with unrepaired DNA damage, leading to severe cell death (Fig. 5C). Whether CHIP-dependent Plk1 ubiquitination would affect cell cycle progression under different stress and the underlying mechanism needs further careful investigation. Since Plk1 is also an HSP90 client protein, we tested whether Plk1 inhibition affects the efficacy of HSP90 inhibitor as well. As described, a combined inhibition of Plk1 and HSP90 enhanced apoptosis in a synergistic manner in multiple PCa cell lines (Fig. 5). Accumulating evidence supports the notion that Plk1 is a valid target for overcoming therapy resistance in PCa. For example, inhibition of Plk1 enhances the efficacy of enzalutamide in both cultured cells and PDX tumors, as Plk1 inhibition prevents activation of the PI3K/AKT/mTOR pathway, which acts upstream of cholesterol biosynthesis, a mechanism to drive AR pathway reactivation (26). Inhibition of Plk1 also overcomes the resistance to metformin, a promising drug for CRPC treatment (50), as Plk1 clearly promotes aerobic glycolysis (51). Finally, we recently showed that combination of inhibition of Plk1 and the WNT/β-catenin pathway is a valid approach to treat CRPC, as Plk1 phosphorylation of Axin2 contributes to inactivation of the WNT/β-catenin pathway (52).

In summary, HSP90 and Plk1 are two promising targets to treat enzalutamide-resistant CRPC. In the absence of HSP90 inhibitor 17-AAG, CHIP-associated ubiquitin ligase activity is inhibited, a stable AR/HSP90/Plk1 complex will lead to stabilized AR and Plk1,

thus contributing to PCa progression. Upon 17-AAG treatment, the AR/HSP90/Plk1 complex is likely to be destabilized, free AR and Plk1 will go through CHIP-dependent ubiquitination, followed by protein degradation. Altogether, a combination of enzalutamide, HSP90 inhibitor 17-AAG, and Plk1 inhibitor BI2536 will likely achieve the best therapeutic outcome.

Supplementary Material

Refer to Web version on PubMed Central for supplementary material.

Acknowledgments

We appreciate Sandra Torregrosa-Allen and Benjamin Ramsey for their help with xenograft study.

Grant Support: This work was supported by NIH grants R01 CA157429 (X. Liu), R01 CA192894 (X. Liu), R01 AR059130 (N. Ahmad), and R01 CA176748 (N. Ahmad).

References

1. Matsumoto T, Sakari M, Okada M, Yokoyama A, Takahashi S, Kouzmenko A, et al. The androgen receptor in health and disease. Annual review of physiology. 2013; 75:201–24.
2. Foley C, Mitsiades N. Moving Beyond the Androgen Receptor (AR): Targeting AR-Interacting Proteins to Treat Prostate Cancer. Hormones & cancer. 2016
3. Gudziak MR, Smith AY. Hormonal therapy for stage D cancer of the prostate. Western Journal of Medicine. 1994; 160:351–9. [PubMed: 8023485]
4. Perlmutter MA, Lepor H. Androgen Deprivation Therapy in the Treatment of Advanced Prostate Cancer. Reviews in Urology. 2007; 9:S3–S8. [PubMed: 17387371]
5. Karantanos T, Corn PG, Thompson TC. Prostate cancer progression after androgen deprivation therapy: mechanisms of castrate resistance and novel therapeutic approaches. Oncogene. 2013; 32:5501–11. [PubMed: 23752182]
6. Lonergan PE, Tindall DJ. Androgen receptor signaling in prostate cancer development and progression. Journal of Carcinogenesis. 2011; 10:20. [PubMed: 21886458]
7. Attard G, Cooper CS, de Bono JS. Steroid hormone receptors in prostate cancer: a hard habit to break? Cancer cell. 2009; 16:458–62. [PubMed: 19962664]
8. Marques RB, Dits NF, Erkens-Schulze S, van Weerden WM, Jenster G. Bypass mechanisms of the androgen receptor pathway in therapy-resistant prostate cancer cell models. PLoS One. 2010; 5:e13500. [PubMed: 20976069]
9. Claessens F, Helsen C, Prekovic S, Van den Broeck T, Spans L, Van Poppel H, et al. Emerging mechanisms of enzalutamide resistance in prostate cancer. Nat Rev Urol. 2014; 11:712–6. [PubMed: 25224448]
10. Tyagi N, Tyagi R. The wonderous chaperones: A highlight on therapeutics of cancer and potentially malignant disorders. Journal of Oral and Maxillofacial Pathology : JOMFP. 2015; 19:212–20. [PubMed: 26604499]
11. Tatokoro M, Koga F, Yoshida S, Kihara K. Heat shock protein 90 targeting therapy: state of the art and future perspective. EXCLI Journal. 2015; 14:48–58. [PubMed: 26600741]
12. Neckers L. Heat shock protein 90: the cancer chaperone. Journal of biosciences. 2007; 32:517–30. [PubMed: 17536171]
13. Lyman SK, Crawley SC, Gong R, Adamkewicz JI, McGrath G, Chew JY, et al. High-Content, High-Throughput Analysis of Cell Cycle Perturbations Induced by the HSP90 Inhibitor XL888. PLoS ONE. 2011; 6:e17692. [PubMed: 21408192]
14. Feldman BJ, Feldman D. The development of androgen-independent prostate cancer. Nat Rev Cancer. 2001; 1:34–45. [PubMed: 11900250]

15. Solit DB, Scher HI, Rosen N. Hsp90 as a therapeutic target in prostate cancer. Seminars in Oncology. 2003; 30:709–16. [PubMed: 14571418]
16. Centenera MM, Fitzpatrick AK, Tilley WD, Butler LM. Hsp90: Still a viable target in prostate cancer. Biochimica et Biophysica Acta (BBA) - Reviews on Cancer. 2013; 1835:211–8. [PubMed: 23287571]
17. DeBoer C, Meulman PA, Wnuk RJ, Peterson DH. Geldanamycin, a new antibiotic. The Journal of antibiotics. 1970; 23:442–7. [PubMed: 5459626]
18. Mimnaugh EG, Chavany C, Neckers L. Polyubiquitination and proteasomal degradation of the p185c-erbB-2 receptor protein-tyrosine kinase induced by geldanamycin. J Biol Chem. 1996; 271:22796–801. [PubMed: 8798456]
19. Saif MW, Erlichman C, Dragovich T, Mendelson D, Toft D, Burrows F, et al. Open-label, dose-escalation, safety, pharmacokinetic, and pharmacodynamic study of intravenously administered CNF1010 (17-(allylamino)-17-demethoxygeldanamycin [17-AAG]) in patients with solid tumors. Cancer chemotherapy and pharmacology. 2013; 71:1345–55. [PubMed: 23564374]
20. Whitesell L, Lin NU. HSP90 as a platform for the assembly of more effective cancer chemotherapy. Biochimica et biophysica acta. 2012; 1823:756–66. [PubMed: 22222203]
21. Gartner EM, Silverman P, Simon M, Flaherty L, Abrams J, Ivy P, et al. A phase II study of 17-allylamino-17-demethoxygeldanamycin in metastatic or locally advanced, unresectable breast cancer. Breast cancer research and treatment. 2012; 131:933–7. [PubMed: 22083229]
22. Pacey S, Gore M, Chao D, Banerji U, Larkin J, Sarker S, et al. A Phase II trial of 17-allylamino, 17-demethoxygeldanamycin (17-AAG, tanespimycin) in patients with metastatic melanoma. Investigational new drugs. 2012; 30:341–9. [PubMed: 20683637]
23. He S, Smith DL, Sequeira M, Sang J, Bates RC, Proia DA. The HSP90 inhibitor ganetespib has chemosensitizer and radiosensitizer activity in colorectal cancer. Investigational new drugs. 2014; 32:577–86. [PubMed: 24682747]
24. Petronczki M, Lénárt P, Peters JM. Polo on the Rise—from Mitotic Entry to Cytokinesis with Plk1. Developmental Cell. 2008; 14:646–59. [PubMed: 18477449]
25. Strebhardt K. Multifaceted polo-like kinases: drug targets and antitargets for cancer therapy. Nature reviews Drug discovery. 2010; 9:643–60. [PubMed: 20671765]
26. Zhang Z, Hou X, Shao C, Li J, Cheng JX, Kuang S, et al. Plk1 inhibition enhances the efficacy of androgen signaling blockade in castration-resistant prostate cancer. Cancer Res. 2014; 74:6635–47. [PubMed: 25252916]
27. Chen YJ, Lai KC, Kuo HH, Chow LP, Yih LH, Lee TC. HSP70 colocalizes with PLK1 at the centrosome and disturbs spindle dynamics in cells arrested in mitosis by arsenic trioxide. Arch Toxicol. 2014; 88:1711–23. [PubMed: 24623308]
28. Chen YJ, Lin YP, Chow LP, Lee TC. Proteomic identification of Hsp70 as a new Plk1 substrate in arsenic trioxide-induced mitotically arrested cells. Proteomics. 2011; 11:4331–45. [PubMed: 21887822]
29. de Carcer G. Heat shock protein 90 regulates the metaphase-anaphase transition in a polo-like kinase-dependent manner. Cancer Res. 2004; 64:5106–12. [PubMed: 15289312]
30. Connell P, Ballinger CA, Jiang J, Wu Y, Thompson LJ, Hohfeld J, et al. The co-chaperone CHIP regulates protein triage decisions mediated by heat-shock proteins. Nat Cell Biol. 2001; 3:93–6. [PubMed: 11146632]
31. Kundrat L, Regan L. Identification of residues on Hsp70 and Hsp90 ubiquitinated by the cochaperone CHIP. Journal of molecular biology. 2010; 395:587–94. [PubMed: 19913553]
32. Muller P, Ruckova E, Halada P, Coates PJ, Hrstka R, Lane DP, et al. C-terminal phosphorylation of Hsp70 and Hsp90 regulates alternate binding to co-chaperones CHIP and HOP to determine cellular protein folding/degradation balances. Oncogene. 2013; 32:3101–10. [PubMed: 22824801]
33. He B, Bai S, Hnat AT, Kalman RI, Minges JT, Patterson C, et al. An androgen receptor NH2-terminal conserved motif interacts with the COOH terminus of the Hsp70-interacting protein (CHIP). J Biol Chem. 2004; 279:30643–53. [PubMed: 15107424]
34. Rees I, Lee S, Kim H, Tsai FT. The E3 ubiquitin ligase CHIP binds the androgen receptor in a phosphorylation-dependent manner. Biochimica et biophysica acta. 2006; 1764:1073–9. [PubMed: 16725394]

35. Sarkar S, Brautigan DL, Parsons SJ, Larner JM. Androgen receptor degradation by the E3 ligase CHIP modulates mitotic arrest in prostate cancer cells. Oncogene. 2014; 33:26–33. [PubMed: 23246967]
36. Beausoleil SA, Jedrychowski M, Schwartz D, Elias JE, Villen J, Li J, et al. Large-scale characterization of HeLa cell nuclear phosphoproteins. Proceedings of the National Academy of Sciences of the United States of America. 2004; 101:12130–5. [PubMed: 15302935]
37. Kuruma H, Matsumoto H, Shiota M, Bishop J, Lamoureux F, Thomas C, et al. A novel antiandrogen, Compound 30, suppresses castration-resistant and MDV3100-resistant prostate cancer growth in vitro and in vivo. Molecular cancer therapeutics. 2013; 12:567–76. [PubMed: 23493310]
38. Centenera MM, Carter SL, Gillis JL, Marrocco-Tallarigo DL, Grose RH, Tilley WD, et al. Co-targeting AR and HSP90 suppresses prostate cancer cell growth and prevents resistance mechanisms. Endocrine-Related Cancer. 2015; 22:805–18. [PubMed: 26187127]
39. Rodriguez-Vida A, Galazi M, Rudman S, Chowdhury S, Sternberg CN. Enzalutamide for the treatment of metastatic castration-resistant prostate cancer. Drug Design, Development and Therapy. 2015; 9:3325–39.
40. Li Y, Chan SC, Brand LJ, Hwang TH, Silverstein KA, Dehm SM. Androgen receptor splice variants mediate enzalutamide resistance in castration-resistant prostate cancer cell lines. Cancer Res. 2013; 73:483–9. [PubMed: 23117885]
41. Bento CF, Fernandes R, Ramalho J, Marques C, Shang F, Taylor A, et al. The Chaperone-Dependent Ubiquitin Ligase CHIP Targets HIF-1α for Degradation in the Presence of Methylglyoxal. PLoS ONE. 2010; 5:e15062. [PubMed: 21124777]
42. Esser C, Scheffner M, Hohfeld J. The chaperone-associated ubiquitin ligase CHIP is able to target p53 for proteasomal degradation. J Biol Chem. 2005; 280:27443–8. [PubMed: 15911628]
43. Li L, Xin H, Xu X, Huang M, Zhang X, Chen Y, et al. CHIP mediates degradation of Smad proteins and potentially regulates Smad-induced transcription. Molecular and cellular biology. 2004; 24:856–64. [PubMed: 14701756]
44. Neckers L, Workman P. Hsp90 molecular chaperone inhibitors: are we there yet? Clinical cancer research : an official journal of the American Association for Cancer Research. 2012; 18:64–76. [PubMed: 22215907]
45. Senn H, Shapiro RS, Cowen LE. Cdc28 provides a molecular link between Hsp90, morphogenesis, and cell cycle progression in Candida albicans. Molecular biology of the cell. 2012; 23:268–83. [PubMed: 22090345]
46. Shang Y, Xu X, Duan X, Guo J, Wang Y, Ren F, et al. Hsp70 and Hsp90 oppositely regulate TGF-beta signaling through CHIP/Stub1. Biochemical and biophysical research communications. 2014; 446:387–92. [PubMed: 24613385]
47. Kang D, Chen J, Wong J, Fang G. The checkpoint protein Chfr is a ligase that ubiquitinates Plk1 and inhibits Cdc2 at the G2 to M transition. The Journal of cell biology. 2002; 156:249–60. [PubMed: 11807090]
48. Metzger T, Kleiss C, Sumara I. CUL3 and protein kinases: insights from PLK1/KLHL22 interaction. Cell Cycle. 2013; 12:2291–6. [PubMed: 24067371]
49. Beck J, Maerki S, Posch M, Metzger T, Persaud A, Scheel H, et al. Ubiquitylation-dependent localization of PLK1 in mitosis. Nat Cell Biol. 2013; 15:430–9. [PubMed: 23455478]
50. Shao C, Ahmad N, Hodges K, Kuang S, Ratliff T, Liu X. Inhibition of Polo-like Kinase 1 (Plk1) Enhances the Antineoplastic Activity of Metformin in Prostate Cancer. Journal of Biological Chemistry. 2015; 290:2024–33. [PubMed: 25505174]
51. Li Z, Li J, Bi P, Lu Y, Burcham G, Elzey BD, et al. Plk1 Phosphorylation of PTEN Causes a Tumor-Promoting Metabolic State. Molecular and cellular biology. 2014
52. Li J, Karki A, Hodges KB, Ahmad N, Zoubeidi A, Strebhardt K, et al. Cotargeting Polo-Like Kinase 1 and the Wnt/beta-Catenin Signaling Pathway in Castration-Resistant Prostate Cancer. Molecular and cellular biology. 2015; 35:4185–98. [PubMed: 26438599]

Abbreviations

HSP	heat shock protein
Plk1	polo-like kinase 1
CRPC	castration-resistant prostate cancer
PCa	prostate cancer
AR	androgen receptor
ADT	androgen deprivation therapy
CHIP	C-terminus of Hsc70 interacting protein
ARE	androgen response elements
GA	geldanamycin
17-AAG	17-allylamino-17-demethoxy-geldanamycin
PSA	prostate specific antigen
IB	immunoblotting
IP	immunoprecipitation
IF	immunofluorescence

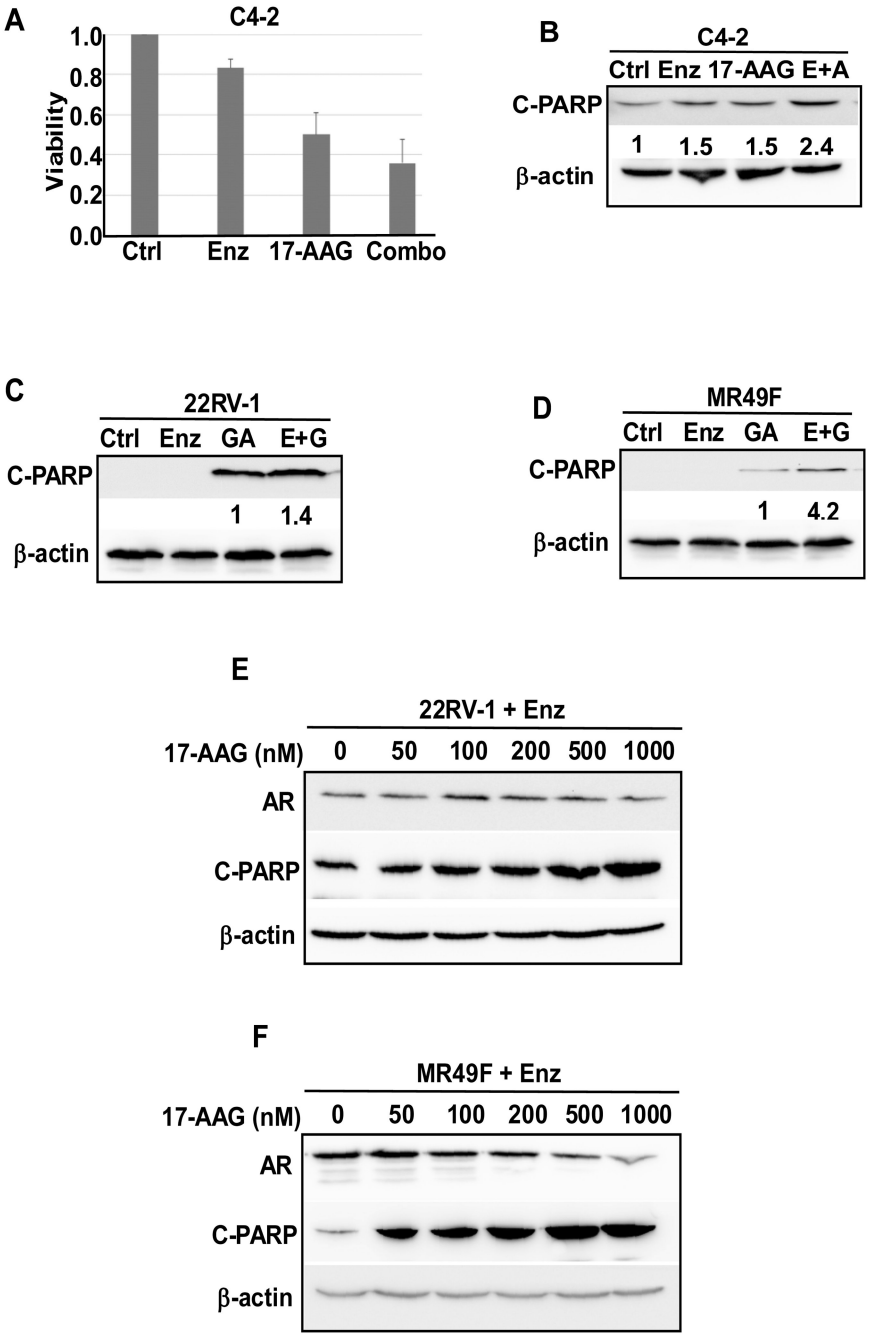

Figure 1.

Combination of AR antagonist enzalutamide and HSP90 inhibitors led to decreased cell viability and increased cell death. (A). C4-2 cells were treated as indicated for 3 days and harvested for cell viability assay. (B) C4-2 cells were treated as indicated for 24 hr, followed by immunoblotting (IB) against cleaved-PARP [Poly(ADP-ribose) polymerase-1)]. (C&D) 22RV1 (C) and MR49F (D) cells were treated as indicated for 24 hr, followed by IB against cleaved-PARP. (E&F) 22RV1 (E) and MR49F (F) cells were treated as indicated with

enzalutamide (10 μM) and indicated increased concentrations of 17-AAG for 24 hr, followed by IB against cleaved-PARP and AR.

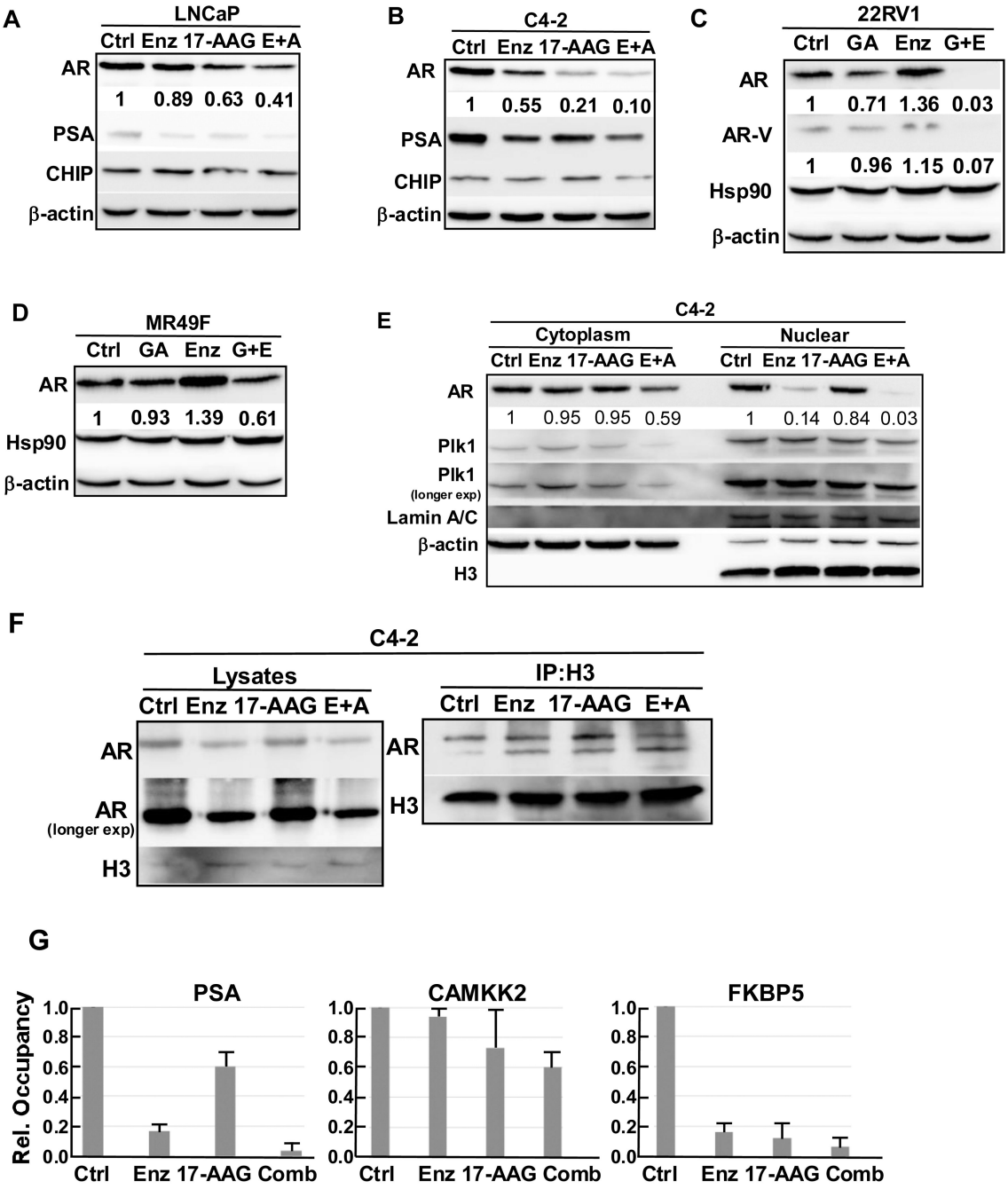

Figure 2.

Combination of enzalutamide and 17-AAG led to decreased AR protein level and transcriptional activity. (A&B) LNCaP (A) and C4-2 (B) cells were treated as indicated for 24 hr, followed by IB against AR, PSA and CHIP. (C&D) 22RV1 (C) and MR49F (D) cells were treated as indicated for 24 hr, followed by IB against AR and HSP90. (E) C4-2 cells were treated as indicated for 24 hr, fractionated into cytoplasm and nuclear, followed by IB against AR and Plk1. (F) C4-2 cells were treated as indicated for 24 hr, and crosslinked with 1% formaldehyde. The chromatin fraction was separated and subjected to anti-histone H3

immunoprecipitation (IP), followed by IB against AR. (G) C4-2 cells were treated as indicated for 24 hr and subjected for CHIP analysis using AR antibody. Binding of AR to the promoter region of PSA, CAMKK2 and FKBP5 were measured using RT-PCR with specific primers targeting the promoter region of indicated genes.

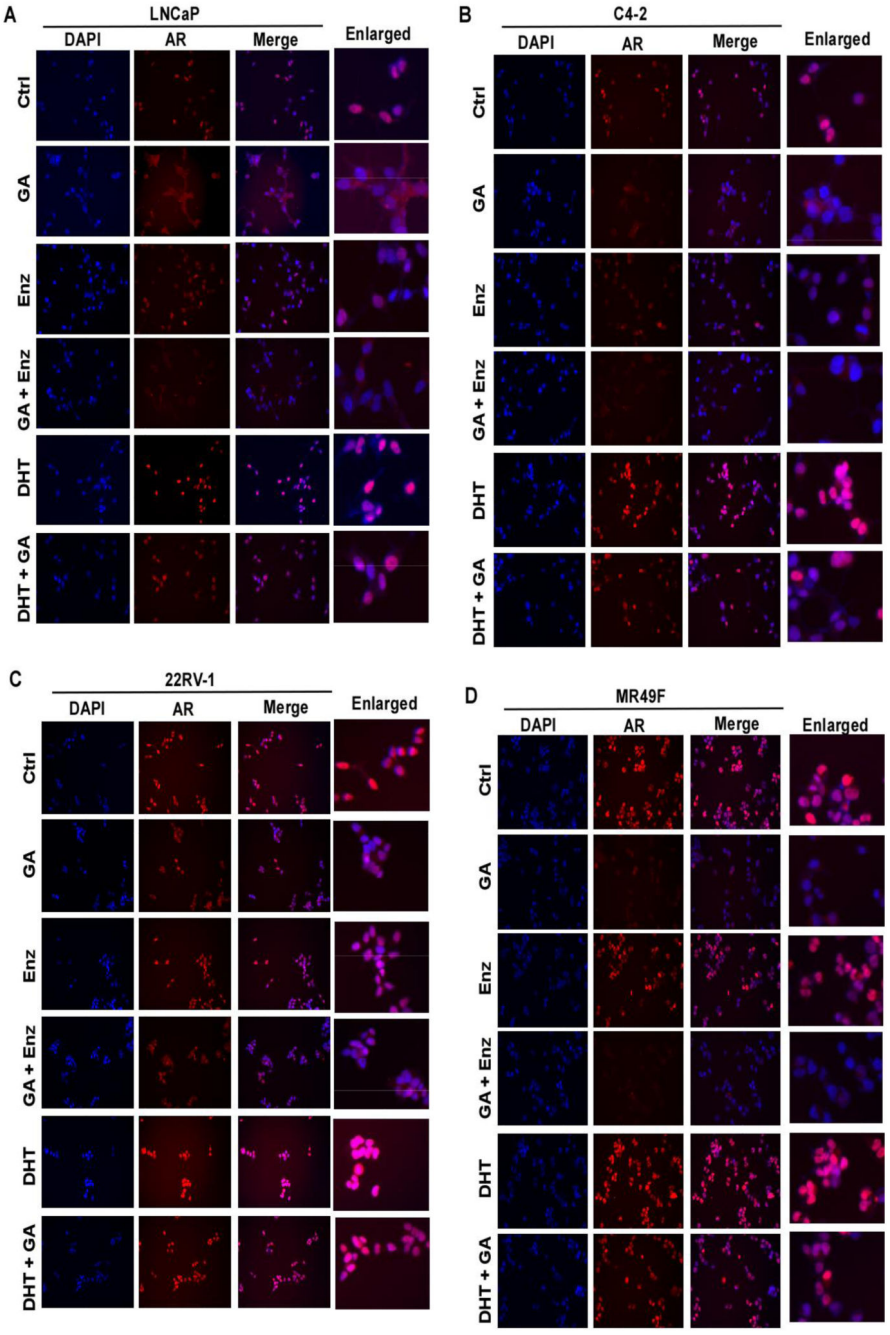

Figure 3.

Combination of enzalutamide and geldanamycin led to cytoplasmic localization of AR. (**a-d**) LNCaP (A), C4-2 (B), 22RV1 (C) and MR49F (D) cells were treated as indicated for 24 hr, then subjected for immunofluorescence (IF) staining against AR.

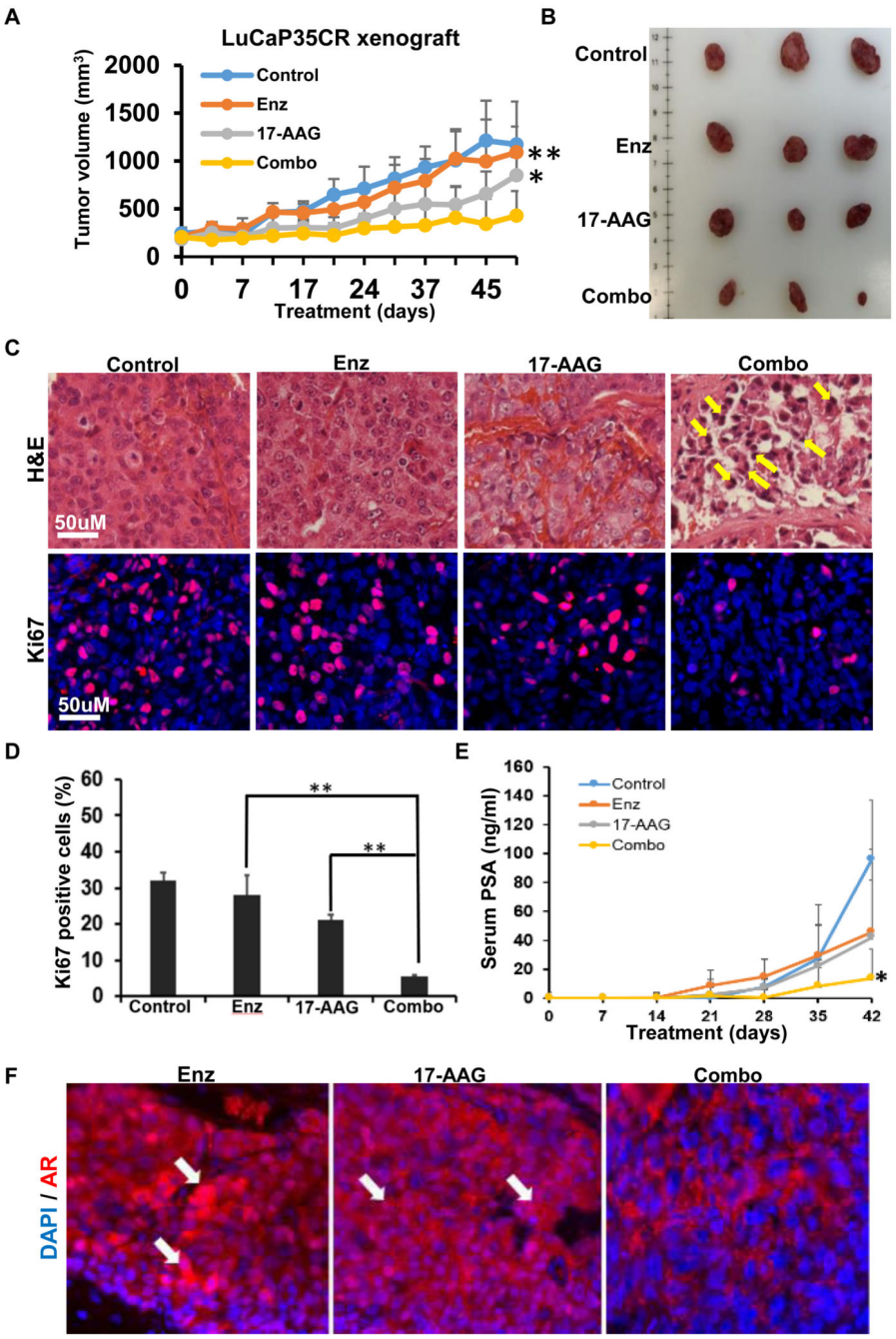

Figure 4.

Combination of enzalutamide and 17-AAG inhibited LuCaP35CR xenograft tumor growth in a synergistic manner. (A) nude mice bearing LuCaP35CR tumors were gavaged with enzalutamide (25 mg/kg) and intraperitoneally injected with 17-AAG (20 mg/kg), either alone or together as indicated, followed for 52 days. **, $P < 0.01$ compared with enzalutamide treatment group on day 52, *, $P < 0.1$ compared with 17-AAG treatment group on day 52. (B) Tumors from LuCaP35CR xenografts at the end of study. (C) H&E staining and anti-Ki67 immunohistochemistry (IHC) staining of tumor sections. Yellow arrows

indicate apoptotic bodies. (D) Quantification of Ki67 staining. **, $P < 0.01$. (E) Blood was collected once per week from LuCaP35CR mice and serum PSA levels were measured. *, $P < 0.1$ compared with single drug treatment. (F) IHC staining for AR of LuCaP35CR tumors, with white arrows indicating nuclear localization of AR.

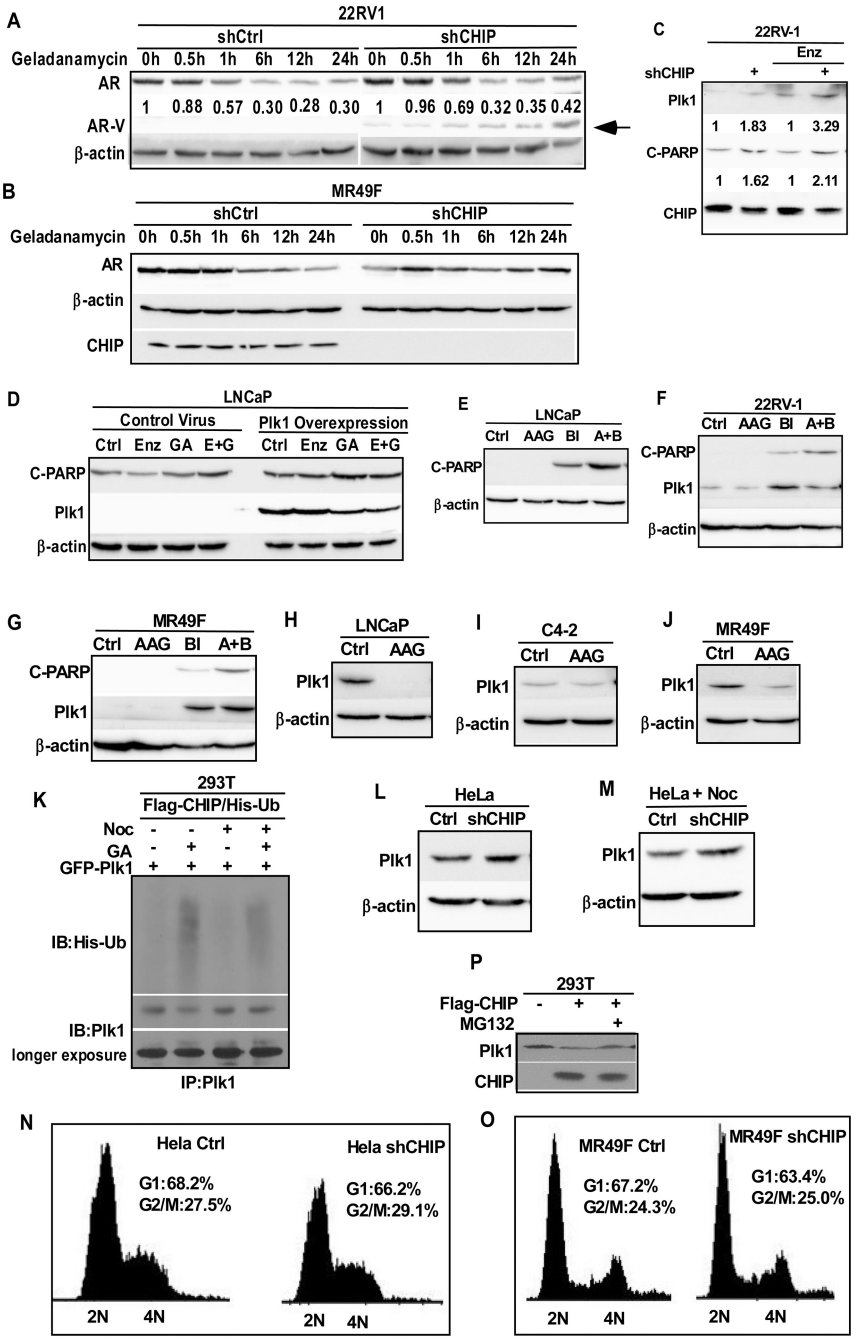

Figure 5.

Plk1 is involved in combination effect of enzalutamide and HSP90 inhibitors. (A) 22RV1 cells were depleted of CHIP using lentivirus-based shRNA, treated with geldanamycin (1 μM) for indicated times and subjected for IB against AR. Arrow indicates the position of AR-V. (B) MR49F cells were depleted of CHIP using lentivirus-based shRNA, treated with geldanamycin (1 μM) for indicated times and subjected for IB against AR. (C) 22RV1 cells were depleted of CHIP, treated as indicated for 24 hr, followed by IB against cleaved-PARP, Plk1 and CHIP. (D) LNCaP cells were infected with lentivirus to overexpress Plk1, treated

as indicated for 24 hr. (E-G) LNCaP (E), 22RV1(F) and MR49F(G) cells were treated as indicated for 24 hr, followed by IB against cleaved PARP. (H-J) LNCaP (H), C4-2 (I) and MR49F (J) cells were treated with 17-AAG (100 nM) for 24 hr and subjected for IB against Plk1. (K) HEK293T cells were co-transfected with Flag-CHIP, His-ubiquitin and GFP-Plk1, treated as indicated for 24 hr, subjected for IP against Plk1, followed by IB against Ubiquitin and Plk1. (L&M) HeLa cells were depleted of CHIP using lentivirus-based shRNA, treated with (M) or without (L) nocodazole (100nM), subjected for IB against Plk1. (N&O) HeLa (N) and MR49F (O) cells were depleted of CHIP using lentivirus-based shRNA and subjected for FACS analysis. Percentages of cells in different cell cycle stage were calculated. (P) HEK293T cells were transfected with Flag-CHIP, treated with MG132 (10 μM) for 6 hr, and subjected for IB against Plk1.

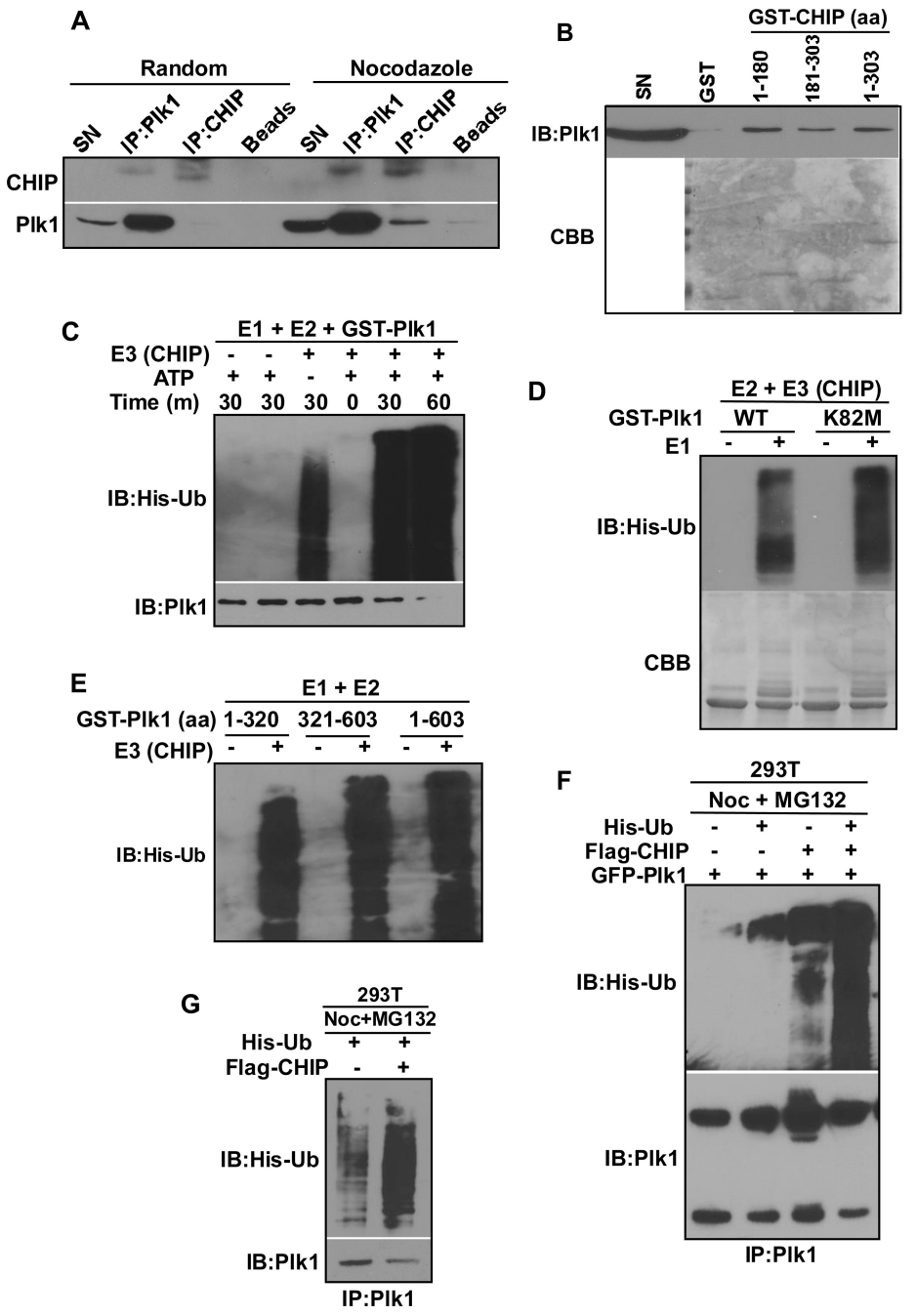

Figure 6.

CHIP ubiquitinates Plk1 in vitro and in cells. (A) Plk1 interacted with CHIP in Hela cells. HeLa cells were treated with or without nocodazole (100nM) and subjected for IP against Plk1 or CHIP, followed by IB against Plk1 and CHIP. (B) Purified GST-CHIP interacted with Plk1 in Hela lysates. N-terminal, C-terminal and full length GST-CHIP proteins were purified with GST beads, incubated with HeLa cell lysates, followed by commassie blue staining (CBB) or IB against Plk1. C-E, CHIP ubiquitinated Plk1 in vitro. (C) In vitro ubiquitination assay of GST-Plk1. GST-Plk1 was incubated with E1, E2, CHIP, HSPs and

ATP for indicated times, followed by IB against Plk1 and ubiquitin. (D) GST-Plk1 (wild type or kinase-dead K82M mutant), purified from insect cells, was subjected for in vitro ubiquitination assay as C for 30 mins. (E) GST-Plk1 fragments were subjected for in vitro ubiquitination assay. (F&G) Overexpression of CHIP led to increased ubiquitination of Plk1 in cells. (F) HEK293T cells were co-transfected with Flag-CHIP, GFP-Plk1 and His-ubiquitin, treated with nocodazole (100nM) for 24 hr and MG132 (10μM) for 6 hr, subjected for IP against Plk1, followed by IB against Plk1 and ubiquitin. (G) HeLa cells were transfected with Flag-CHIP and His-ubiquitin, treated with nocodazole (100nM) for 24 hr and MG132 (10μM) for 6 hr, subjected for anti-Plk1 IP, followed by IB against Plk1 and ubiquitin.

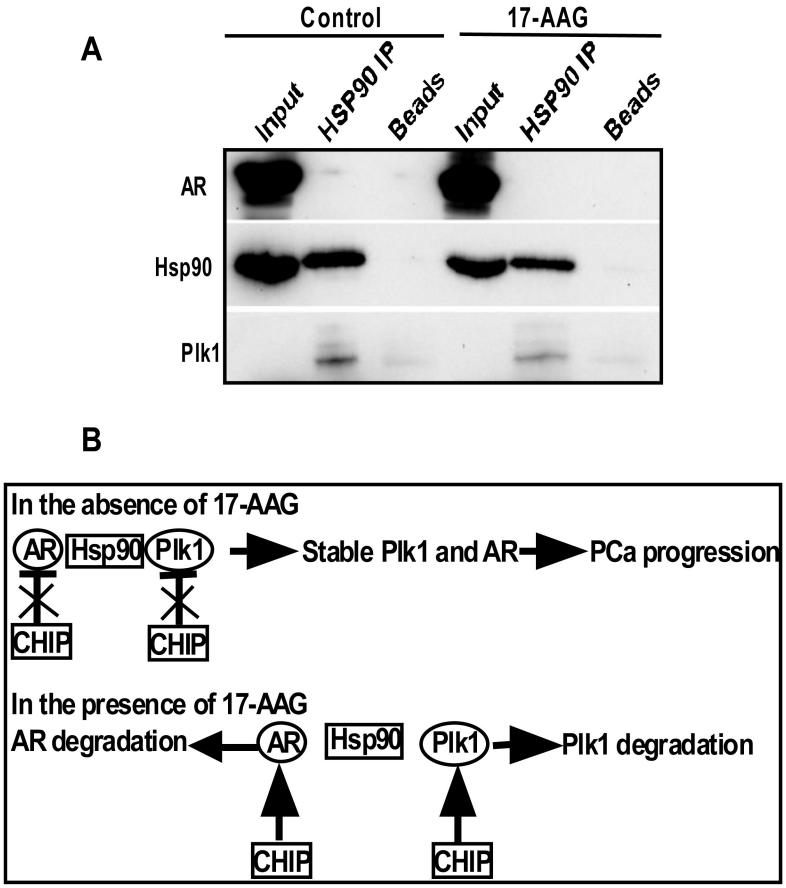

Figure 7.

CHIP-mediated degradation of AR and Plk1 regulates the efficacy of HSP90 inhibitor. (A) LNCaP cells were treated with or without 17-AAG for 24 hr, subjected for IP against HSP90, followed by IB against HSP90, Plk1 and AR. (B) A working model of inhibition of HSP90 signaling pathways.